What is the real origin of activity of Fe-N-C electrocatalysts in O_2 reduction reaction? Critical roles of coordinating pyrrolic N and axially adsorbing species

Xu Hu [1], Suya Chen [1], Letian Chen [1], Yun Tian[2], Sai Yao[1], Zhengyu Lu[1], Xu Zhang[2]*, Zhen Zhou[1,2]*

[1] School of Materials Science and Engineering, Institute of New Energy Material Chemistry, Renewable Energy Conversion and Storage Center (ReCast), Key Laboratory of Advanced Energy Materials Chemistry (Ministry of Education), Nankai University, Tianjin 300350, China

[2] School of Chemical Engineering, Zhengzhou University, Zhengzhou 450001, Henan, China

* Corresponding author. E-mail: zzuzhangxu@zzu.edu.cn; zhouzhen@nankai.edu.cn

1. Supporting Figures

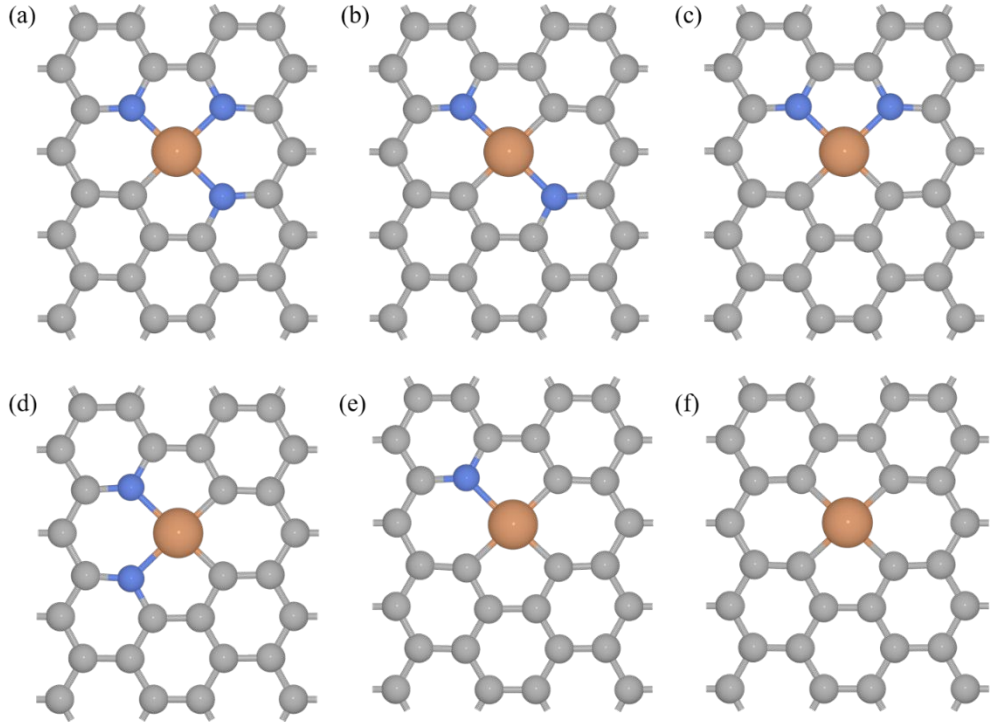

Figure S1. Six different pyridinic N type FeN_xC models. (a) pyridinic FeN_3C, (b) pyridinic FeN_2C-1, (c) pyridinic FeN_2C-2, (d) pyridinic FeN_2C-3, (e) pyridinic FeN_1C, (f) pyridinic FeN_0C. C, gray; N, blue; Fe, brown.

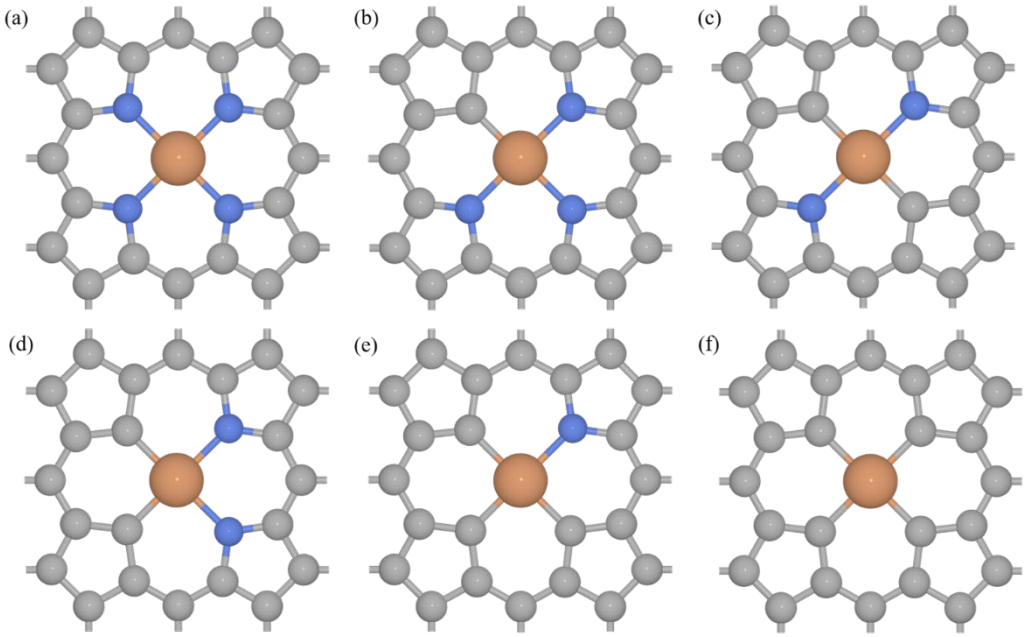

Figure S2. Six different pyrrolic N type FeN_xC models. (a) pyrrolic FeN_4C, (b) pyrrolic FeN_3C, (c) pyrrolic FeN_2C-1, (d) pyrrolic FeN_2C-2, (e) pyrrolic FeN_1C, (f) pyrrolic FeN_0C. C, gray; N, blue; Fe, brown.

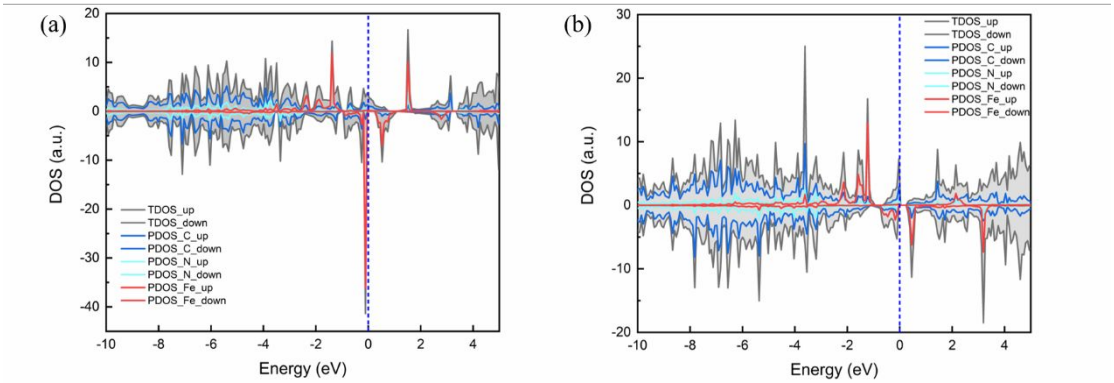

Figure S3. Density of state analysis diagram of (a) pyrrolic and (b) pyridinic FeN_4C. The blue dashed line represents the Fermi level.

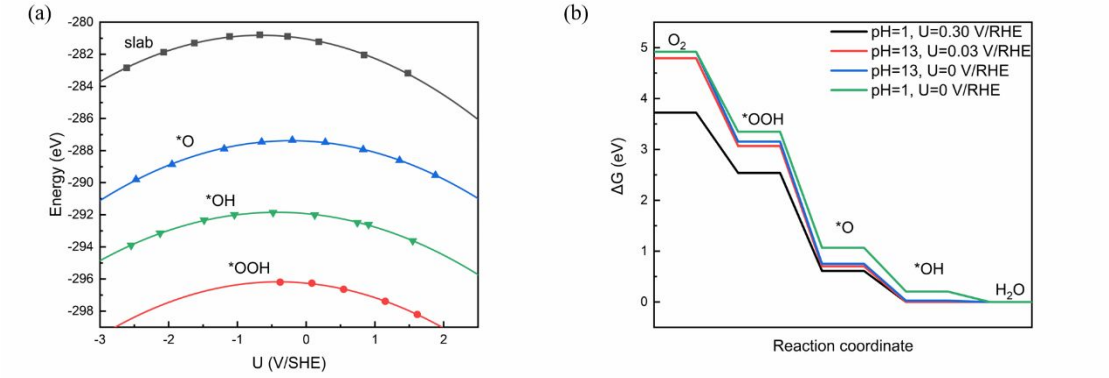

Figure S4. (a) The calculated energies of bare pyridinic FeN_3C slab (black) and corresponding three reaction intermediates (*OOH, red; *O, blue; *OH, green) as a function of applied electrode potential. (b) Free energy profile of ORR catalyzed by pyridinic FeN_3C at U = 0.30 V/RHE, pH = 1; U = 0.03 V/RHE, pH = 13; U = 0 V/RHE, pH = 13; and U = 0 V/RHE, pH = 1.

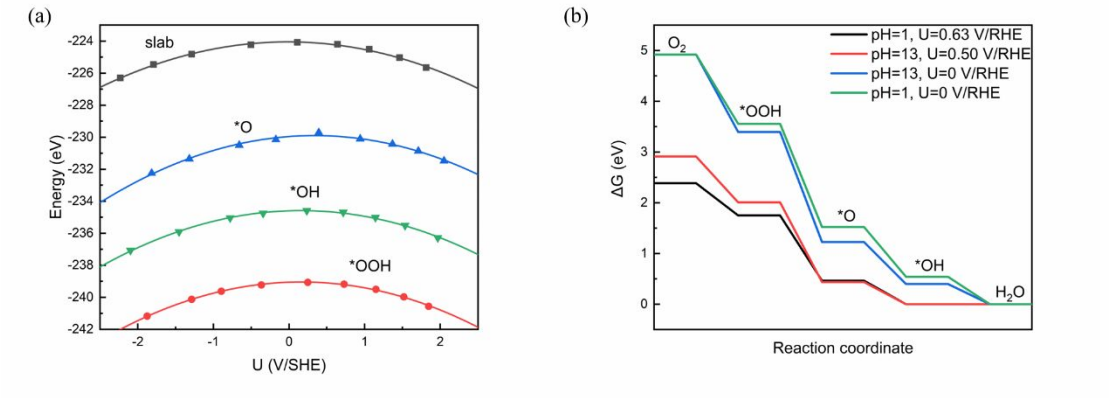

Figure S5. (a) The calculated energies of bare pyrrolic FeN_3C slab (black) and corresponding three reaction intermediates (*OOH, red; *O, blue; *OH, green) as a function of applied electrode potential. (b) Free energy profile of ORR catalyzed by pyrrolic FeN_3C at U = 0.63 V/RHE, pH = 1; U = 0.50 V/RHE, pH = 13; U = 0 V/RHE, pH = 13; and U = 0 V/RHE, pH = 1.

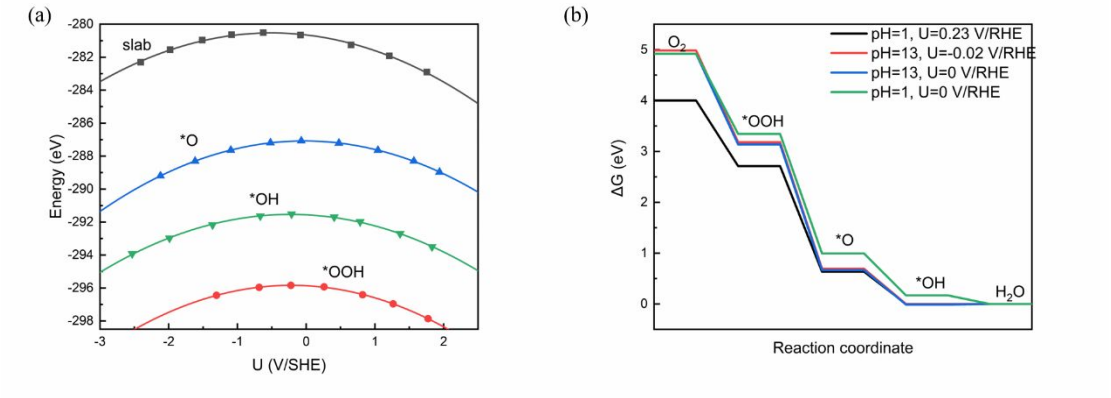

Figure S6. (a) The calculated energies of bare pyridinic FeN_2C-2 slab (black) and corresponding three reaction intermediates (*OOH, red; *O, blue; *OH, green) as a function of applied electrode potential. (b) Free energy profile of ORR catalyzed by pyridinic FeN_2C-2 at U = 0.23 V/RHE, pH = 1; U = -0.02 V/RHE, pH = 13; U = 0 V/RHE, pH = 13; and U = 0 V/RHE, pH = 1.

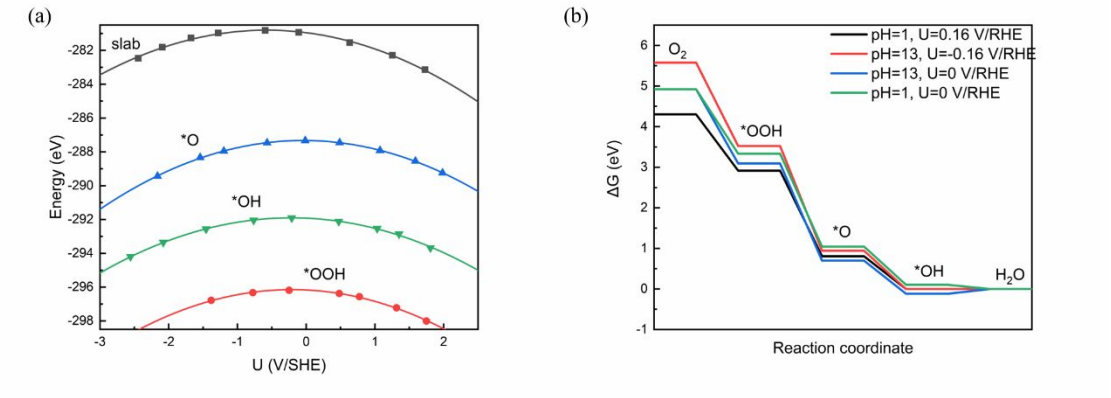

Figure S7. (a) The calculated energies of bare pyridinic FeN_2C-3 slab (black) and corresponding three reaction intermediates (*OOH, red; *O, blue; *OH, green) as a function of applied electrode potential. (b) Free energy profile of ORR catalyzed by pyridinic FeN_2C-3 at U = 0.16 V/RHE, pH = 1; U = -0.16 V/RHE, pH = 13; U = 0 V/RHE, pH = 13; and U = 0 V/RHE, pH = 1.

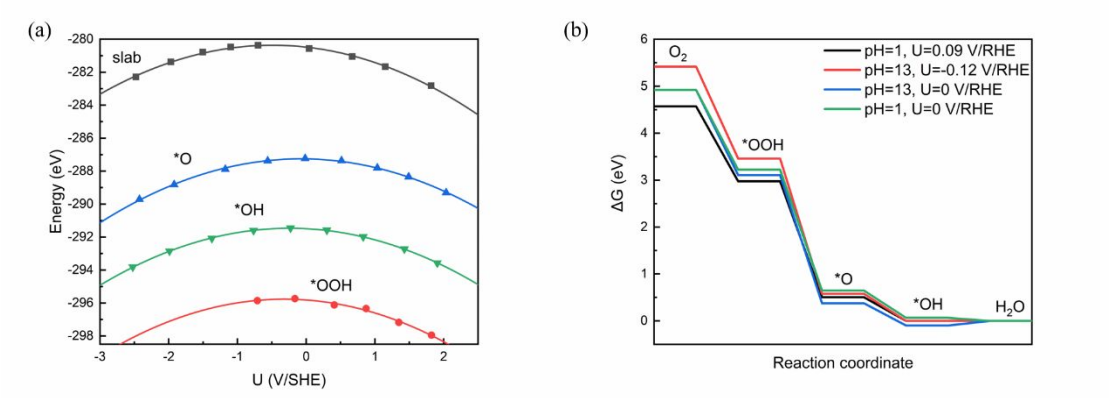

Figure S8. (a) The calculated energies of bare pyridinic FeN_2C-1 slab (black) and corresponding three reaction intermediates (*OOH, red; *O, blue; *OH, green) as a function of applied electrode potential. (b) Free energy profile of ORR catalyzed by pyridinic FeN_2C-1 at U = 0.09 V/RHE, pH = 1; U = -0.12 V/RHE, pH = 13; U = 0 V/RHE, pH = 13; and U = 0 V/RHE, pH = 1.

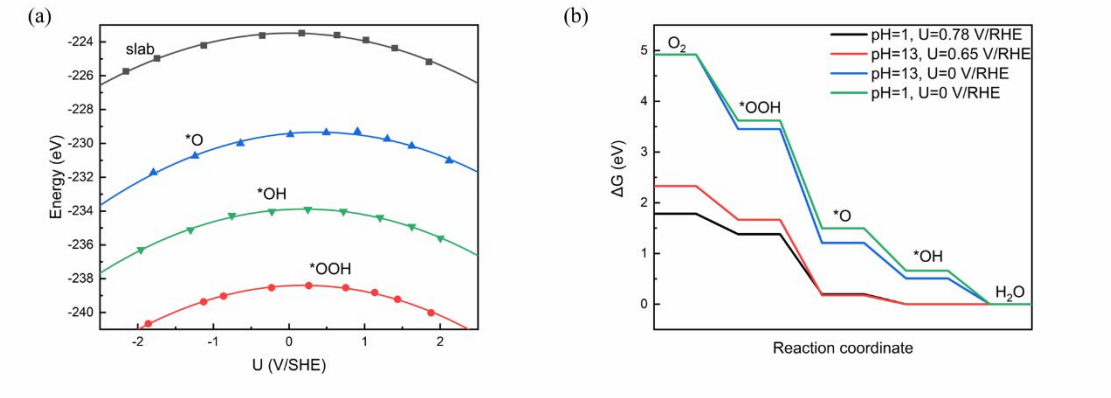

Figure S9. (a) The calculated energies of bare pyrrolic FeN_2C-2 slab (black) and corresponding three reaction intermediates (*OOH, red; *O, blue; *OH, green) as a function of applied electrode potential. (b) Free energy profile of ORR catalyzed by pyrrolic FeN_2C-2 at U = 0.78 V/RHE, pH = 1; U = 0.65 V/RHE, pH = 13; U = 0 V/RHE, pH = 13; and U = 0 V/RHE, pH = 1.

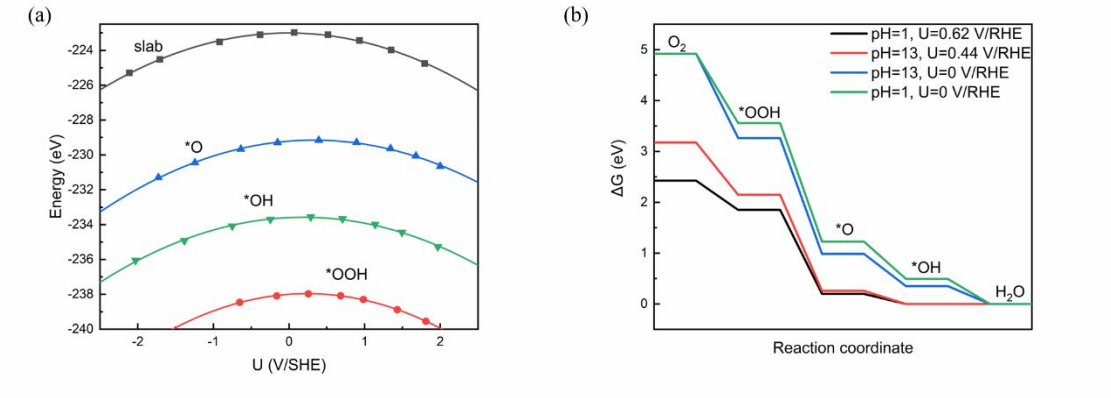

Figure S10. (a) The calculated energies of bare pyrrolic FeN_2C-1 slab (black) and corresponding three reaction intermediates (*OOH, red; *O, blue; *OH, green) as a function of applied electrode potential. (b) Free energy profile of ORR catalyzed by pyrrolic FeN_2C-1 at U = 0.62 V/RHE, pH = 1; U = 0.44 V/RHE, pH = 13; U = 0 V/RHE, pH = 13; and U = 0 V/RHE, pH = 1.

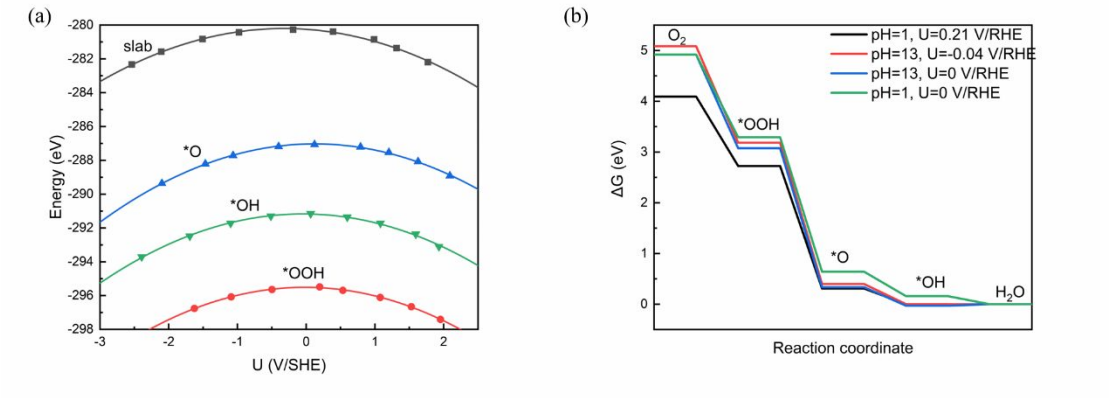

Figure S11. (a) The calculated energies of bare pyridinic FeN_1C slab (black) and corresponding three reaction intermediates (*OOH, red; *O, blue; *OH, green) as a function of applied electrode potential. (b) Free energy profile of ORR catalyzed by pyridinic FeN_0C at U = 0.21 V/RHE, pH = 1; U = -0.04 V/RHE, pH = 13; U = 0 V/RHE, pH = 13; and U = 0 V/RHE, pH = 1.

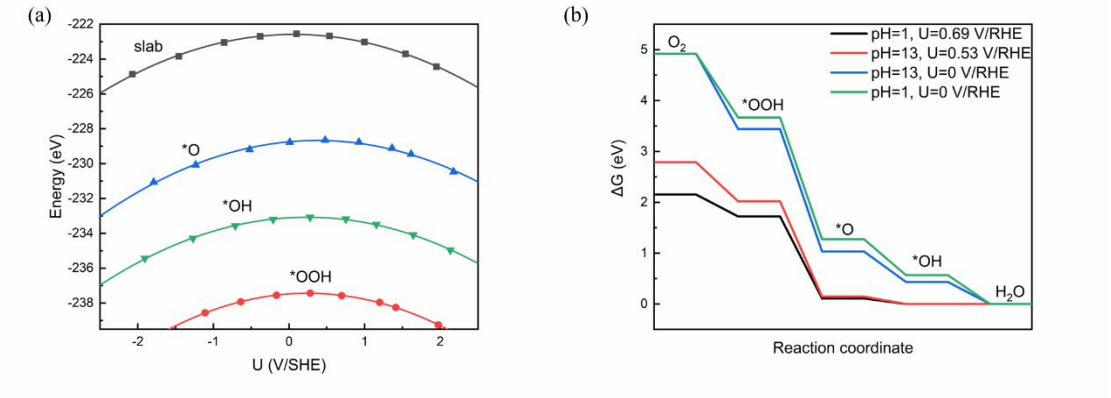

Figure S12. (a) The calculated energies of bare pyrrolic FeN_1C slab (black) and corresponding three reaction intermediates (*OOH, red; *O, blue; *OH, green) as a function of applied electrode potential. (b) Free energy profile of ORR catalyzed by pyrrolic FeN_1C at U = 0.69 V/RHE, pH = 1; U = 0.53 V/RHE, pH = 13; U = 0 V/RHE, pH = 13; and U = 0 V/RHE, pH = 1.

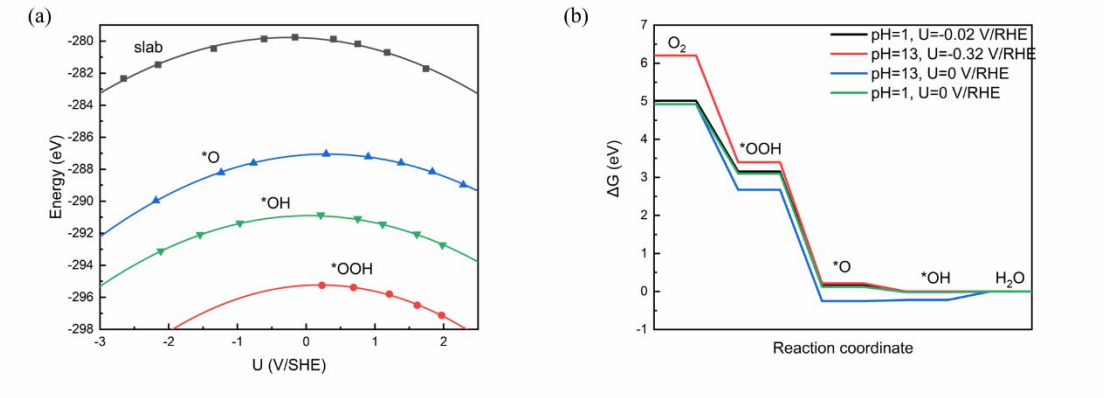

Figure S13. (a) The calculated energies of bare pyridinic FeN_0C slab (black) and corresponding three reaction intermediates (*OOH, red; *O, blue; *OH, green) as a function of applied electrode potential. (b) Free energy profile of ORR catalyzed by pyridinic FeN_0C at U = -0.02 V/RHE, pH = 1; U = -0.32 V/RHE, pH = 13; U = 0 V/RHE, pH = 13; and U = 0 V/RHE, pH = 1.

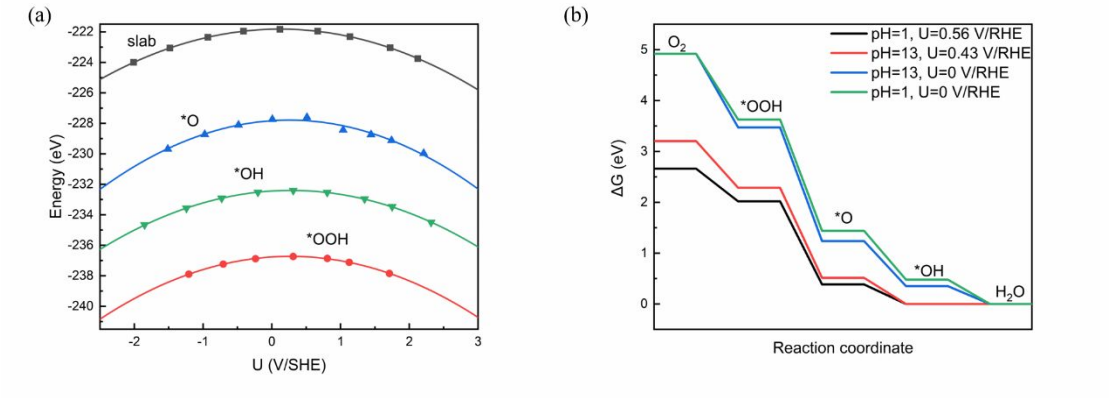

Figure S14. (a) The calculated energies of bare pyrrolic FeN_0C slab (black) and corresponding three reaction intermediates (*OOH, red; *O, blue; *OH, green) as a function of applied electrode potential. (b) Free energy profile of ORR catalyzed by pyrrolic FeN_0C at U = 0.56 V/RHE, pH = 1; U = 0.43 V/RHE, pH = 13; U = 0 V/RHE, pH = 13; and U = 0 V/RHE, pH = 1.

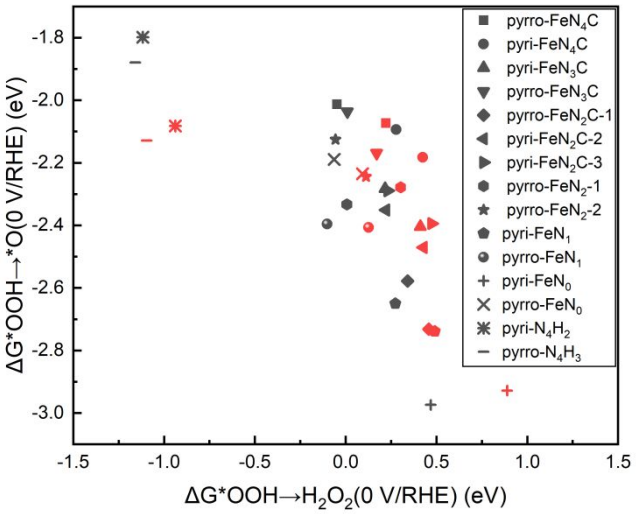

Figure S15. The free energy change for H_2O_2 formation and *O formation at 0 V/RHE under pH =1 (black symbol) or 13 (red symbol) for different configurations. "pyri" means pyridinic and "pyrro" means pyrrolic.

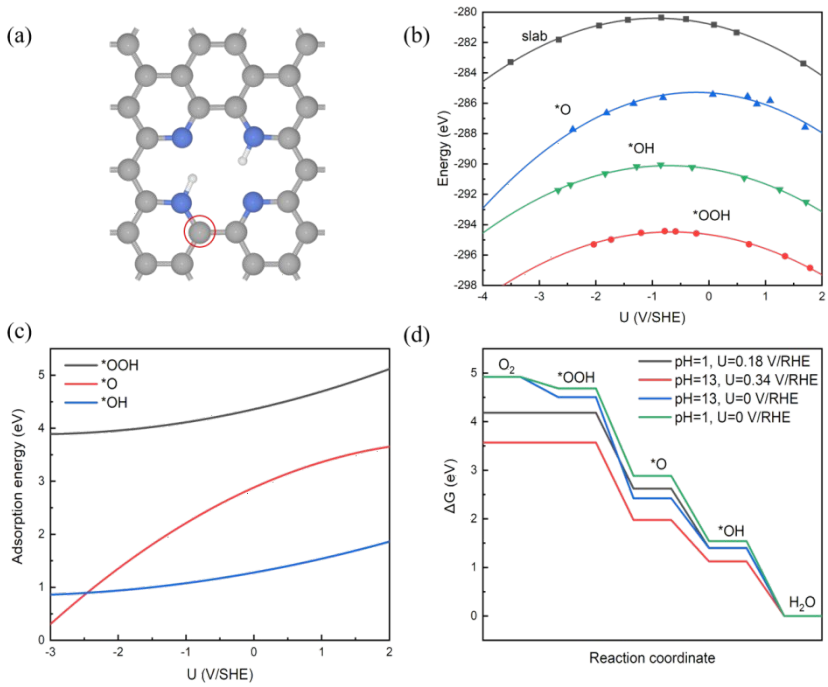

Figure S16. (a) Optimized structure of pyridinic-N_4H_2. The active site is marked by red circle. (b) The calculated energies of bare pyridinic N_4H_2 slab (black) and corresponding three reaction intermediates (*OOH, red; *O, blue; *OH, green) as a function of applied electrode potential. (c) The adsorption energies of *OOH, *O, and *OH as a function of applied electrode potential. (d) Free energy profile of ORR catalyzed by pyridinic N_4H_2 at U = 0.18 V/RHE, pH = 1; U = 0.34 V/RHE, pH = 13; U = 0 V/RHE, pH = 13; and U = 0 V/RHE, pH = 1. C, gray; N, blue; H, white.

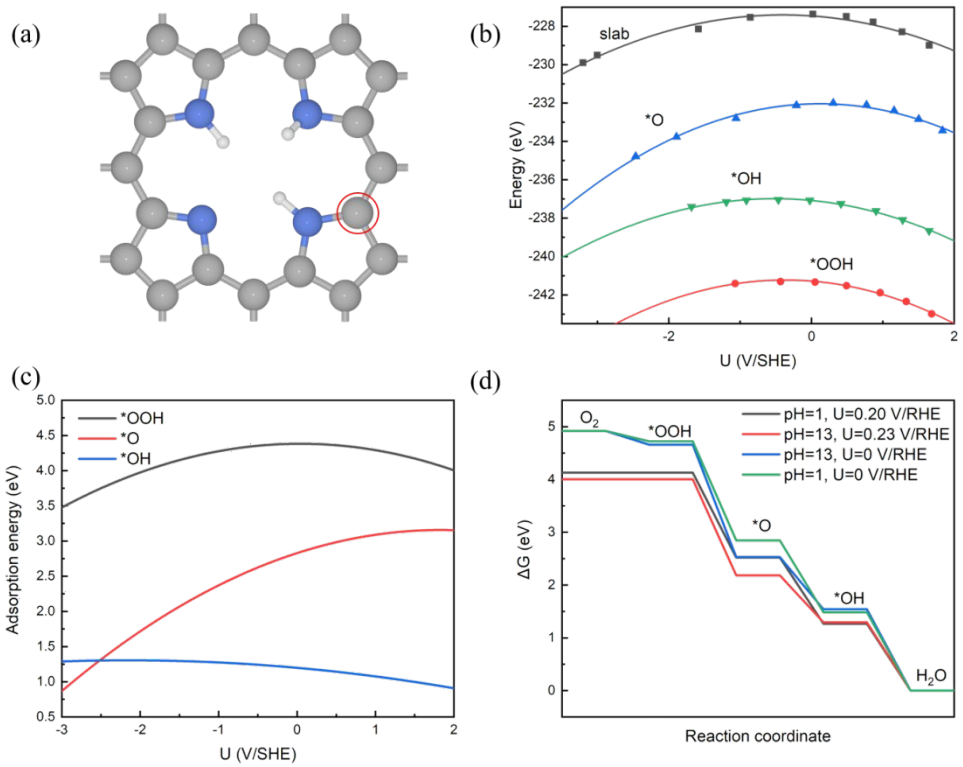

Figure S17. (a) Optimized structure of pyrrolic N_4H_3. The active site is marked by red circle. (b) The calculated energies of bare pyrrolic N_4H_3 slab (black) and corresponding three reaction intermediates (*OOH, red; *O, blue; *OH, green) as a function of applied electrode potential. (c) The adsorption energies of *OOH, *O, and *OH as a function of applied electrode potential. (d) Free energy profile of ORR catalyzed by pyrrolic N_4H_3 at U = 0.20 V/RHE, pH = 1; U = 0.23 V/RHE, pH = 13; U = 0 V/RHE, pH = 13; and U = 0 V/RHE, pH = 1. C, gray; N, blue; H, white.

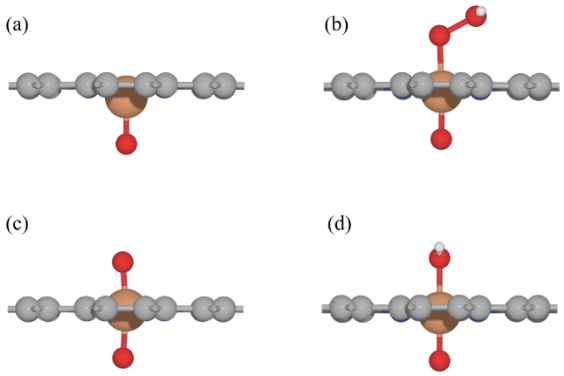

Figure S18. Optimized reaction models during the ORR catalyzed by pyridinic *O-FeN_4C at zero excess charge case. C, gray; N, blue; O, red; H, white, Fe, brown.

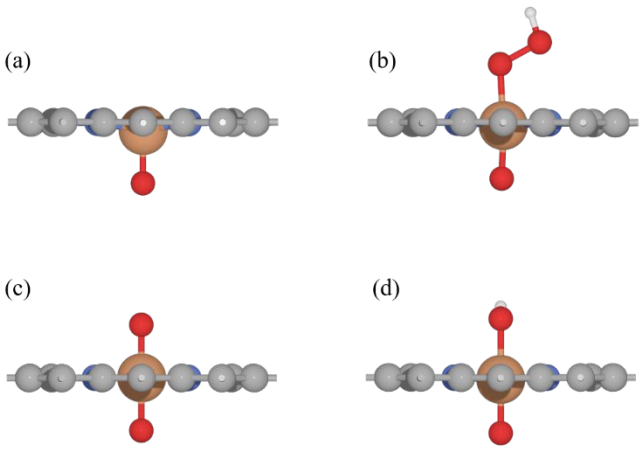

Figure S19. Optimized reaction models during the ORR catalyzed by pyrrolic *O-FeN_4C at zero excess charge case. C, gray; N, blue; O, red; H, white, Fe, brown.

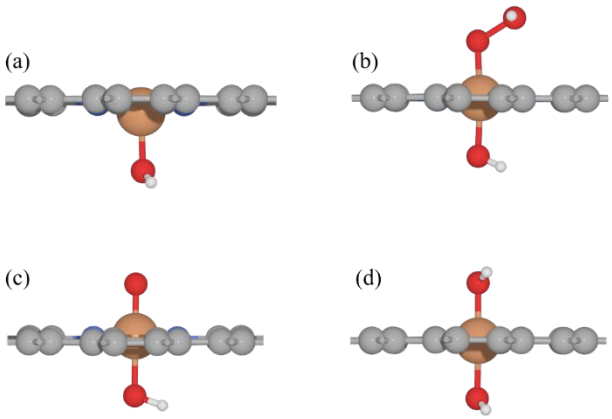

Figure S20. Optimized reaction models during the ORR catalyzed by pyridinic *OH-FeN_4C at zero excess charge case. C, gray; N, blue; O, red; H, white, Fe, brown.

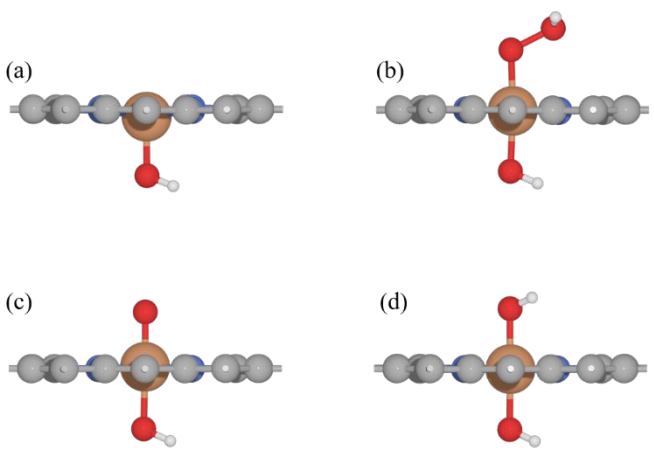

Figure S21. Optimized reaction models during the ORR catalyzed by pyrrolic *OH-FeN_4C at zero excess charge case. C, gray; N, blue; O, red; H, white, Fe, brown.

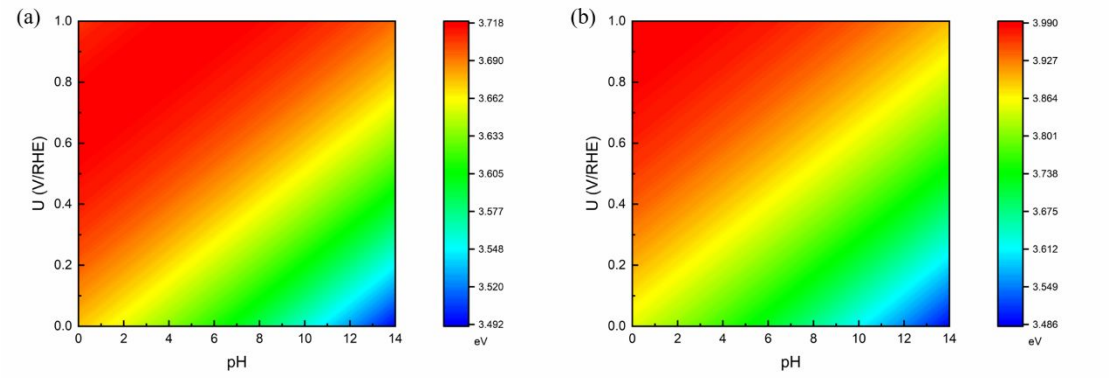

Figure S22. pH-dependent and potential-dependent contour plot of adsorption energies of *OOH on (a) pyridinic and (b) pyrrolic *O-FeN_4C.

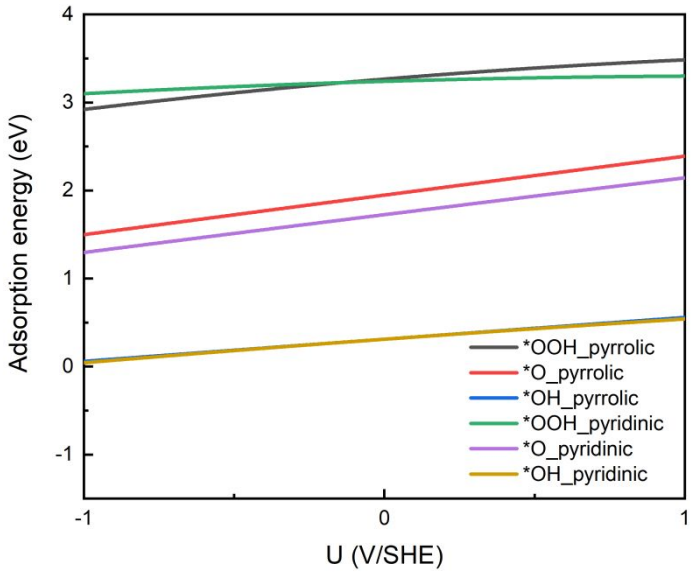

Figure S23. The adsorption energies of *OOH, *O, and *OH as a function of applied potential on pyridinic *OH-FeN_4C and pyrrolic *OH-FeN_4C.

2. Supporting tables

Table S1. The DFT energies (E(DFT)) and corresponding free energy correction values (ΔG) of H_2(g) and H_2O(l) are calculated at 1 bar and 0.035 bar. Due to the fact that O_2 is poorly described in DFT calculations, the free energy of O_2 is calculated by $G_{O_2} = 2G_{H_2O} - 2G_{H_2} + 4.921$ eV. The DFT energies of H_2 and H_2O were calculated in a 10 Å × 10 Å × 10 Å unit cell in vacuum.

	pressure/bar	temperature/K	E(DFT)/eV	ΔG/eV	G/eV
O_2(g)	1	298.150	/	/	-9.903
H_2(g)	1	298.150	-6.771	-0.040	-6.811
H_2O(l)	0.035	298.150	-14.223	0.000	-14.223

Table S2. Fitted parameters of the potential-dependent free energy (with the from $E = I+b_1\times U+b_2\times U^2$) for pyridinic FeN_4C. U_0 (V/SHE) and C (e/V) are the potential of zero charge (PZC) and capacitance of the corresponding system, respectively, and E_0 (eV) is the energy of the system at the PZC.

Species	I	b_1	b_2	C	U_0	E_0	R^2
slab	-281.410	-0.831	-0.537	1.074	-0.773	-281.089	0.9990
***OOH**	-296.681	-0.605	-0.516	1.031	-0.587	-296.503	0.9982
***O**	-287.645	-0.451	-0.480	0.959	-0.470	-287.539	0.9978
***OH**	-292.109	-0.635	-0.489	0.978	-0.649	-291.903	0.9976

Table S3. Fitted parameters of the potential-dependent free energy for pyrrolic FeN_4C.

Species	I	b_1	b_2	C	U_0	E_0	R^2
slab	-224.772	-0.113	-0.395	0.790	-0.143	-224.764	0.9916
***OOH**	-239.713	0.168	-0.515	1.031	0.162	-239.699	0.9538
***O**	-230.599	0.277	-0.486	0.971	0.285	-230.559	0.9944
***OH**	-235.034	0.081	-0.517	1.035	0.079	-235.031	0.9864

Table S4. Fitted parameters of the potential-dependent free energy for pyridinic *O-FeN_4C.

Species	I	b_1	b_2	C	U_0	E_0	R^2
slab	-287.645	-0.451	-0.480	0.959	-0.470	-287.539	0.9978
***OOH**	-302.201	-0.316	-0.581	1.162	-0.272	-302.158	0.9990
***O**	-292.411	-0.136	-0.533	1.066	-0.128	-292.402	0.9973
***OH**	-297.747	-0.213	-0.496	0.993	-0.214	-297.725	0.9975

Table S5. Fitted parameters of the potential-dependent free energy for pyrrolic *O-FeN_4C.

Species	I	b_1	b_2	C	U_0	E_0	R^2
slab	-230.599	0.277	-0.486	0.971	0.285	-230.559	0.9944
***OOH**	-244.980	0.578	-0.646	1.292	0.447	-244.851	0.9904
***O**	-235.223	0.648	-0.560	1.119	0.579	-235.035	0.9999
***OH**	-240.508	0.635	-0.577	1.155	0.550	-240.333	0.9990

Table S6. Fitted parameters of the potential-dependent free energy for pyridinic *OH-FeN_4C.

Species	I	b_1	b_2	C	U_0	E_0	R^2
slab	-292.109	-0.635	-0.489	0.978	-0.649	-291.903	0.9976
***OOH**	-307.099	-0.535	-0.529	1.059	-0.505	-306.964	0.9996
***O**	-297.796	-0.211	-0.494	0.988	-0.213	-297.774	0.9980
***OH**	-302.617	-0.386	-0.507	1.015	-0.380	-302.543	0.9956

Table S7. Fitted parameters of the potential-dependent free energy for pyrrolic *OH-FeN_4C.

Species	I	b_1	b_2	C	U_0	E_0	R^2
slab	-235.034	0.081	-0.517	1.035	0.079	-235.031	0.9864
***OOH**	-249.998	0.363	-0.581	1.161	0.312	-249.941	0.9968
***O**	-240.499	0.527	-0.521	1.042	0.506	-240.366	0.9842
***OH**	-245.541	0.330	-0.520	1.039	0.318	-245.488	0.9949

Table S8. Fitted parameters of the potential-dependent free energy for pyridinic FeN_3C.

Species	I	b_1	b_2	C	U_0	E_0	R^2
slab	-281.049	-0.692	-0.520	1.040	-0.665	-280.819	0.9984
***OOH**	-296.255	-0.402	-0.499	0.999	-0.402	-296.175	0.9993
***O**	-287.406	-0.218	-0.484	0.968	-0.226	-287.382	0.9988
***OH**	-291.924	-0.385	-0.454	0.908	-0.424	-291.842	0.9989

Table S9. Fitted parameters of the potential-dependent free energy for pyrrolic FeN_3C.

Species	I	b_1	b_2	C	U_0	E_0	R^2
slab	-224.049	-0.014	-0.459	0.919	-0.015	-224.049	0.9959
***OOH**	-239.054	0.167	-0.517	1.033	0.161	-239.040	0.9979
***O**	-229.958	0.351	-0.520	1.040	0.337	-229.899	0.9877
***OH**	-234.596	0.155	-0.498	0.997	0.155	-234.584	0.9973

Table S10. Fitted parameters of the potential-dependent free energy for pyridinic FeN_2C-2.

Species	I	b_1	b_2	C	U_0	E_0	R^2
slab	-280.650	-0.479	-0.474	0.949	-0.505	-280.529	0.9958
***OOH**	-295.862	-0.220	-0.513	1.025	-0.215	-295.839	0.9996
***O**	-287.081	-0.029	-0.484	0.969	-0.030	-287.081	0.9999
***OH**	-291.562	-0.211	-0.458	0.916	-0.230	-291.538	0.9989

Table S11. Fitted parameters of the potential-dependent free energy for pyridinic FeN_2C-3.

Species	I	b_1	b_2	C	U_0	E_0	R^2
slab	-280.948	-0.514	-0.448	0.896	-0.573	-280.801	0.9940
***OOH**	-296.168	-0.197	-0.476	0.952	-0.207	-296.148	0.9975
***O**	-287.327	-0.040	-0.465	0.930	-0.043	-287.326	0.9994
***OH**	-291.922	-0.181	-0.420	0.841	-0.215	-291.902	0.9980

Table S12. Fitted parameters of the potential-dependent free energy for pyridinic FeN_2C-1.

Species	I	b_1	b_2	C	U_0	E_0	R^2
slab	-280.479	-0.463	-0.471	0.943	-0.491	-280.365	0.9958
***OOH**	-295.817	-0.306	-0.480	0.959	-0.319	-295.769	0.9920
***O**	-287.260	-0.067	-0.452	0.905	-0.074	-287.258	0.9980
***OH**	-291.495	-0.219	-0.454	0.908	-0.241	-291.468	0.9996

Table S13. Fitted parameters of the potential-dependent free energy for pyrrolic FeN_2C-2.

Species	I	b_1	b_2	C	U_0	E_0	R^2
slab	-223.479	0.023	-0.483	0.967	0.024	-223.478	0.9938
***OOH**	-238.418	0.208	-0.545	1.090	0.191	-238.398	0.9970
***O**	-229.411	0.394	-0.524	1.047	0.376	-229.337	0.9863
***OH**	-233.904	0.207	-0.520	1.041	0.199	-233.883	0.9971

Table S14. Fitted parameters of the potential-dependent free energy for pyrrolic FeN_2C-1.

Species	I	b_1	b_2	C	U_0	E_0	R^2
slab	-223.004	-0.010	-0.526	1.052	-0.010	-223.004	0.9972
***OOH**	-237.998	0.311	-0.642	1.284	0.242	-237.960	0.9994
***O**	-229.208	0.339	-0.515	1.029	0.330	-229.153	0.9974
***OH**	-233.596	0.196	-0.516	1.032	0.190	-233.577	0.9962

Table S15. Fitted parameters of the potential-dependent free energy for pyridinic FeN_1C.

Species	I	b_1	b_2	C	U_0	E_0	R^2
slab	-280.248	-0.283	-0.438	0.875	-0.323	-280.203	0.9951
***OOH**	-295.512	-0.017	-0.486	0.973	-0.018	-295.512	0.9987
***O**	-287.034	0.117	-0.475	0.950	0.123	-287.026	0.9981
***OH**	-291.172	-0.046	-0.470	0.940	-0.049	-291.171	0.9964

Table S16. Fitted parameters of the potential-dependent free energy for pyrrolic FeN_1C.

Species	I	b_1	b_2	C	U_0	E_0	R^2
slab	-222.588	0.065	-0.513	1.027	0.063	-222.586	0.9981
***OOH**	-237.477	0.308	-0.609	1.218	0.253	-237.438	0.9996
***O**	-228.746	0.393	-0.526	1.051	0.374	-228.673	0.9936
***OH**	-233.106	0.249	-0.519	1.037	0.240	-233.076	0.9991

Table S17. Fitted parameters of the potential-dependent free energy for pyridinic FeN_0C.

Species	I	b_1	b_2	C	U_0	E_0	R^2
slab	-279.805	-0.238	-0.462	0.925	-0.257	-279.774	0.9919
***OOH**	-295.251	0.237	-0.606	1.211	0.196	-295.228	0.9978
***O**	-287.102	0.282	-0.474	0.949	0.297	-287.060	0.9993
***OH**	-290.901	0.040	-0.477	0.954	0.042	-290.901	0.9956

Table S18. Fitted parameters of the potential-dependent free energy for pyrrolic FeN_0C.

Species	I	b_1	b_2	C	U_0	E_0	R^2
slab	-221.829	0.117	-0.480	0.960	0.122	-221.822	0.9999
***OOH**	-236.762	0.290	-0.537	1.073	0.270	-236.723	0.9995
***O**	-227.828	0.303	-0.598	1.196	0.253	-227.790	0.9698
***OH**	-232.438	0.280	-0.500	1.001	0.280	-232.399	0.9999

Table S19. The DFT calculated energy of pure FeN_4C, *O-FeN_4C, *OH-FeN_4C and corresponding configurations after metal dissolution and N protonation, N_4H_x(x=1,2,3,4)

	FeN_4C	*O-FeN_4C	*OH-FeN_4C	N_4H_0	N_4H_1	N_4H_2	N_4H_3	N_4H_4
energy (pyrrolic FeN_4)/eV	-223.775	-229.396	-233.937	-211.148	-216.831	-222.051	-226.134	-229.498
energy (pyridinic FeN_4)/eV	-279.978	-286.200	-290.612	-269.481	-274.542	-279.253	-282.248	-285.134

The most stable N protonation species for pyridinic and pyrrolic N_4H_x are determined by protonation energy change, $\Delta E_{protonation}$ which is defined as $\Delta E_{protonation} = E(N_4H_x) - E(N_4H_0) - x/2E(H_2)$, where $E(N_4H_x)$, $E(N_4H_0)$ and $E(H_2)$ is the DFT calculated energy of N_4H_x, N_4H_0 and H_2. We determine the most stable protonation species for pyridinic and pyrrolic to be N_4H_2 and N_4H_3 by the corresponding minimum $\Delta E_{protonation}$.